The Thesis Committee for Sebastian Muñoz
Certifies that this is the approved version of the following Thesis:

Heat Transport Variability Across the Streambed of a Large, Regulated River Subject to Hydropeaking

APPROVED BY
SUPERVISING COMMITTEE:

M Bayani Cardenas, Supervisor

Daniella M Rempe, Committee Member

David Mohrig, Committee Member

Heat Transport Variability Across the Streambed of A Large, Regulated River Subject to Hydropeaking

by

Sebastian Muñoz

Undergraduate Honors Thesis

Presented to the Jackson School of Geosciences

and

the College of Liberal Arts

of The University of Texas at Austin

in Partial Fulfillment

of the Requirements

for the Degrees of

Bachelor of Science

and

Bachelor of Arts

The University of Texas at Austin

May 2018

Acknowledgements

This work could not have been completed without the dedication, attention to detail, and hard work of many people beyond myself. I would like to thank my graduate student mentor Stephen Ferencz for being a reliable field partner, mentor, outstanding role model, and for taking the time to work closely with me throughout the project. I extend sincerest gratitude to my advisor Dr. M. Bayani Cardenas for mentoring me, encouraging me to pursue hydrogeology, and helping me push my limits. Thanks are also extended to his Co Principal Investigator on the project, Dr. Bethany Neilson at Utah State University for providing funding for the research and for mentoring me from afar through the many skype meetings we had. I would also like to extend thanks to my committee members Drs. David Mohrig and Daniella Rempe for their support, and Drs. Mark Cloos and Jaime Barnes for leading the honors program and getting me involved in research.

I could never express enough thanks to my parents for their unending support and focus on providing me with enriching opportunities and experiences throughout my lifetime. I have always been encouraged to question and think creatively, processes which have been vital in completing this work.

This project was supported by NSF Grants EAR-1344547 and EAR- 1343861, The University of Texas at Austin, and the Utah State University Water Research Laboratory.

Heat Transport Variability Across the Streambed of A Large, Regulated River Subject to Hydropeaking

Sebastian Muñoz,

The University of Texas at Austin, 2018

Supervisor: Meinhard Bayani Cardenas

Abstract:

Dams affect over half of the Earth's large river systems. Storage of water and its release for peak demand (hydropeaking) changes the thermal regime of the river and impacts the surface and groundwater interactions downstream of a dam. Temperature is an important ecological variable influencing fish, invertebrates, microbial communities and nutrient processing, and can also be used as a tracer of groundwater flow in sediment. Despite this importance, little is known about how dams affect temperatures downstream across the river corridor, particularly temperatures in the subsurface. This study investigates the impact on thermal regime and surface and groundwater interactions hydropeaking has on a 4th order dam-regulated river on several spatial scales. Two transects of thermistors recorded temperature gradients in the riverbed over the course of several flood pulses at 5-minute intervals. One transect was across the channel spanning the 68 m from bank-to-bank and the other was along the bank. The cross-channel transect additionally had piezometers with instruments collecting temperature, pressure and electrical conductivity to corroborate temperature measurement interpretations. The findings were that near-bank and in-channel temperature profiles respond differently to hydropeaking. Hydropeaking reverses head gradients daily near the bank and cause the river to fluctuate between gaining and losing water on hour timescales while in the channel, gradient reversals do not occur. Near the bank, stage increases causes warmer

surface water to penetrate into the subsurface and during the receding limb, cooler groundwater upwells as the river returns to base flow conditions. Temperature ranges near the bank in the subsurface exceed those observed in the stream. Flux and gradient reversals localized at the bank explain temperature distributions in the streambed sediments. Temperature differences and ranges near the bank in the subsurface cannot be explained by conduction alone and advective heat transport through groundwater flow provides a mechanism that explains the temperature distributions through time. Evidence from pressure and temperature sensors moving downstream along the bank verify this effect is not only localized to the cross channel transect. These measurements serve as observational evidence for the impact loading from rapid stage change has on subsurface sediments preventing the reversal of pressure gradients in the channel while causing them near the bank. This impact is analogous to tidal fluctuations and has been show in modeling in both marine and freshwater environments.

Table of Contents

List of Figures

1. Introduction

1.1. Problem

Temperature exerts control on ecological processes. Temperature has also been used as a tracer of groundwater and surface water flow. Dams are in place on many large river systems in the world, and their effects on temperature profiles and surface water groundwater interactions downstream remain understudied. Thus, the purpose of this research is to determine how hydropeaking, the storage and intermittent release of river water from reservoirs, affects the subsurface thermal regime and hyporheic surface water groundwater mixing of a 4th order dam regulated river.

1.2. Hypothesis

This study tests the following hypothesis: The warm water associated with an epilimnetic (top of reservoir) release and the pressure changes associated with stage increase will combine to increase heat transport into the stream bed and mixing between surface and groundwater in the stream bed will be visible in temperature profiles.

1.3. Temperature: Ecologically Significant and Useful as a Tracer

Temperature is one of the most important environmental variables affecting aquatic organisms and most aquatic organisms body temperatures fluctuate directly with ambient water temperature (Hester and Doyle, 2011). Therefore, any alteration of the stream or streambed thermal regime can influence a multitude of species. One important effect of temperature is on dissolved oxygen. Water temperature and dissolved oxygen are inversely related such that as temperature increases (decreases), the solubility (and

potential for) dissolved oxygen decreases (increases) (Chapra, 2008), which means temperature can affect species by controlling the availability of dissolved oxygen. Temperature also influences metabolic rates, physiology and life history, and community based processes such as nutrient cycling and productivity (Poole and Berman, 2001). This importance extends from microbial communities to fish and invertebrates and studies have shown that benthic insect assemblages are unrelated to latitude or elevation and rely almost exclusively on temperature (Hawkins et al., 1997). The importance of stream temperature lies in its quality as an overarching ecological variable, and Łaszewski (2016) states the need for further studies on river thermal regimes noting the impact it would have on applied science, aquatic ecology, and fishery management. In addition, the importance of stream thermal regime predicates that anthropogenic stressors impacting stream temperatures cause changes in fish biology and ecology. This has contributed to freshwater fish species becoming some of the most threatened (Parkinson et al., 2016). Observational data has shown that groundwater influences channel water temperatures when it enters the stream channel and cool patches of water can act as thermal refugia for fish and other aquatic organisms (Poole and Berman, 2001; Burkholder et al., 2008; Ebersole et al., 2003).

Beyond its ecological significance, temperature can be used as a tracer for surface and groundwater flow. Determining groundwater flow is most commonly done utilizing Darcy's law

$$q = -K\frac{dh}{dl} \quad (1)$$

where q is specific discharge in m/s which can be multiplied by a cross sectional area to arrive at a volumetric discharge, K is hydraulic conductivity, and $\frac{dh}{dl}$ indicates a change in head over a change in length, also described as a pressure gradient. However, measuring pressure data requires the use of expensive pressure transducers and

installation of piezometers (miniature observational wells). This labor-intensive process of installing wells and cost often impart limitations on the number and resolution of measurements taken. Additionally, hydraulic conductivity depends on sediment texture, must be measured empirically, and is a function dependent on grain size commonly varying several orders of magnitude (Rau et al., 2014). For these reasons, using heat measurements as surrogates for head measurements in estimating ground water fluxes are a useful alternative (Anderson, 2005). In contrast to hydraulic conductivity, thermal conductivities dependence on sediment texture is much better constrained, and does not rely on grain size (Rau et al., 2014). Equation 2 from (Rau et al., 2012) shows that the thermal front velocity is directly proportional to the specific discharge.

$$v^t = \frac{p_w\, c_w}{pc} \times q \tag{2}$$

Where v^t equals thermal front velocity, $p_w\, c_w$ is the specific volumetric heat capacity of water [J/m^3/°C], pc is the specific heat capacity of the bulk volume [J/m^3/°C] and q is specific discharge (m/s). Compared to pressure, temperature is relatively inexpensive and easy to measure in high resolution. Temperature can be utilized as a tracer in surface and groundwater interactions in the streambed, and temperature profiles can reveal circulation and flow patterns. Temperature measurements have been used to identify surface water infiltration, flow through fractures and flow patterns in groundwater basins as well capturing the details of flow in near surface sediments (Anderson, 2005; Conant, 2004).

1.4. The Significance of Dams

Globally, it is estimated that there are at least 45,000 large dams (>15 m in height) with as many as a million smaller dams worldwide (Allan and Castillo, 2007). These dams impact over half of the worlds large river systems, and include the eight most

biogeographically diverse (Nilsson et al., 2005). Dam regulation is often accompanied by hydropeaking—when facilities store water for later which consists of rapidly releasing water producing higher and faster flows that the background low flow state (Jones, 2014). This method produces rivers with a high stage and a low stage, and the ratio between these can determine whether a river is dominated by generalist tolerant species (in the case of a high peak to low flow ratio) or by specialized species (in the case of a low peak to low flow ratio) (Poff et al., 1997).

Dams directly affect downstream river temperatures, and in the case of an epilimnetic dam (releasing from the top of the reservoir) releases are often warmer than the groundwater (Poole and Berman, 2001). This difference can amount to different surface water and groundwater end member temperatures, which can be detected by methods discussed above. Previous work on dams and their effects on surface groundwater exchanges and thermal regimes in large rivers have included (Gerecht et al., 2011), (Sawyer et al., 2009), and (Arntzen et al., 2006). All three studies found that hydro peaking resulted in the temporary reversal of head gradients, driving water into and out of the bed and bank on daily timescales. One limitation of these studies is that observation locations were confined to the nearbank area due to the complexity and logistical difficulty of measuring further into the stream channel. Jones (2014) noted that research investigating the relationship between high and low flows and ecological integrity, system productivity and biodiversity is needed. Arntzen et al. (2006) recognized the need for studies of large scale systems with varying channel morphology, depth of alluvium, and known groundwater discharge zones, and noted the advantages of working in a regulated system where daily fluctuations of 2 m are common since changes occur on a daily rather than seasonal timescale.

1.5. THE IMPORTANCE OF THE HYPORHEIC ZONE

The mixing of surface water and groundwater regulates many chemical reactions in the streambed. Findlay (1995) broadly defines the hyporheic zone as the sediments that are directly hydrologically linked to the open stream channel while Poole and Berman (2001) define it as the portion of the alluvial aquifer that contains at least some hyporheic groundwater. Their definition of hyporheic groundwater is water that enters the alluvial aquifer from the stream and travels along localized subsurface flow pathways for relatively short periods of time without leaving the alluvial aquifer.

Hydropeaking encourages mixing and changes in the thermal regime of subsurface sediments. The work done by Gerecht et al. (2011), Sawyer et al. (2009) and Arntzen et al. (2006) demonstrated some of these effect. Additionally, they showed that gradient reversals occur throughout hydropeaking events, inducing a change in flow direction. These studies also demonstrated that groundwater upwelling can limit the extent of the hyporheic zone.

An ecotone is a transitional zone between two environments, and the hyporheic zone represents the transition between slow moving, nutrient deplete, and temperature stable groundwater and fast moving, nutrient rich, and dynamic surface water. In the hyporheic zone typically the bulk of microbial biomass is in biofilms within sediment (Boano et al., 2014). Hancock (2002) notes the importance of this ecotone as it hosts unique invertebrate fauna and intense biogeochemical activity. Findlay (1995) expands on this concept by introducing the idea that residence times of surface water in the system increase by hyporheic mixing. The additional time spent in the river bed allow more time for reactions to take place. A study done by Trauth et al., (2018) found that the highest rates of denitrification occur when infiltrated river water fraction and hyporheic

temperatures are high, and determined that interactions between rivers and groundwater are likely key controls on nitrate removal.

The chemical gradient in the hyporheic zone is one from oxic surface water near a downwelling zone where river water infiltrates, to anoxic groundwater conditions along deeper portions of a flow path. At the end of its path, reintroduction to the surface mixes the now anoxic (or partially anoxic) hyporheic waters with oxic surface waters. This distribution of oxygen implies renewal of biologically produced organic carbon (as opposed to carbon locked up in minerals) at depth, as the uptake of O_2 implies the presence of microbial organisms (Findlay, 1995). Strong redox gradients occur at in the interface between surface and groundwater due to microbial activity. In the hyporheic zone typically the bulk of microbial biomass is in biofilms within sediment (Boano et al., 2014). Oxygen is used biologically as a terminal electron acceptor (TEAP) during respiration of organic matter, and as it is depleted, microbial communities that can use other TEAPs such as nitrate, manganese, and iron flourish. This causes a mosaic of electron acceptors and donors to exists that are spatially and temporally heterogeneous and in flux with the constantly changing conditions in the hyporheic zone (Dahm et al., 1998).

Hyporheic zone development potential is a function of channel water hydraulics and groundwater hydraulics (White, 1993) which can be influenced by temperature and pressure differences induced by dam regulations. These factors enforce the necessity of understanding the changing physical and chemical characteristics that results from dam regulation yet hyporheic zones in large rivers remain understudied due to the logistical difficulties in instrumenting and data collection on meaningful scales. Several workers have acknowledged the need for more studies describing the role that river stage changes

have on the mixing of surface water and groundwater in the riverbed (Vervier et al., 1992;Curry et al., 1994 ;Gerecht et al., 2011).

1.6. STUDY SITE

The lower Colorado River near the City of Austin is a regulated fourth order river that is managed by the Lower Colorado River Authority (LCRA). The study site is

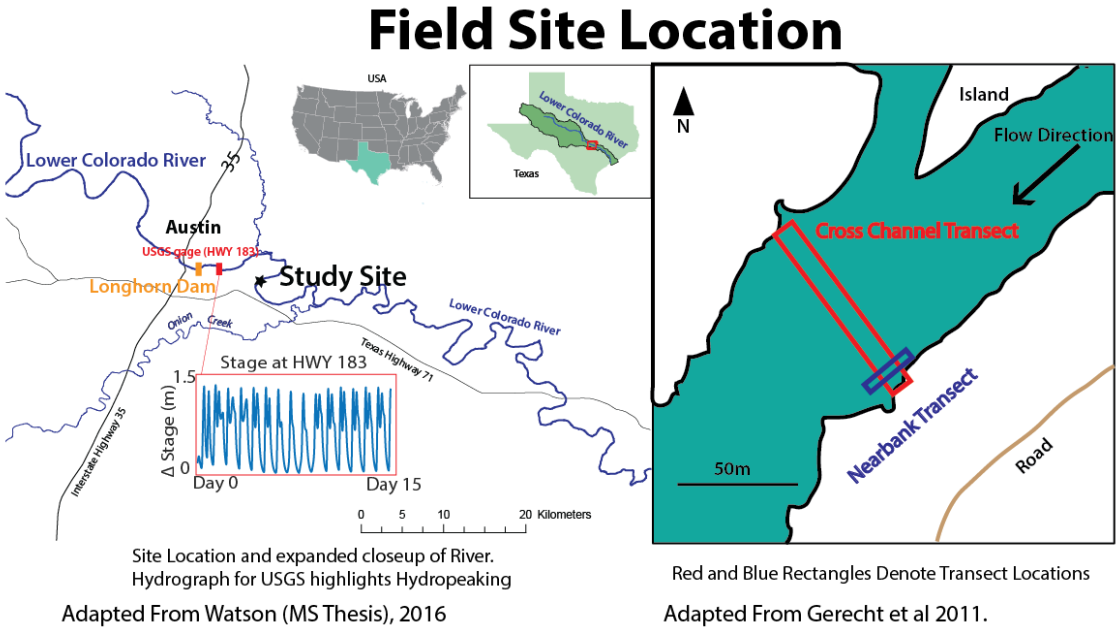

Figure 1. Study site locality, proximity to Austin, USGS gauge data and a close-up of the field site.

located 14km downstream of Longhorn Dam and is shown in Figure 1. Longhorn Dam is the last dam in a series of six dams that regulate discharge along the lower Colorado River. This network of dams are used for flood prevention and provide water for over 1 million people ("LCRA dams form the Highland Lakes"). Conveniently, there is a USGS gauge 12 km upstream of the study site (2 km downstream from Longhorn Dam) that records discharge and stage every 15 minutes. The USGS gauge webpage reports the

watershed draining 71,500 km^2 upstream of the gauge and shows the river stage at this location had daily fluctuations of least 1.5 meters throughout the summer of 2017 due to dam operations (U.S. Geological Survey, 2018). The dam is an epilimnetic spill-over design that empties the shallow, dammed Lady Bird Lake near Austin, Texas. Because of this design, the water released from the dam is warm, ranging from 26-30 °C during the summer. During the summer months, when this study was conducted, there is typically a large contrast of 7-10 °C between the surface water and groundwater temperatures. This combination of proximity to a hydropeaked dam, large temperature difference between surface and groundwater, and large catchment size makes the lower Colorado River an ideal natural laboratory for investigating the effects of hydropeaking on surface and groundwater interactions in a large river.

2. Methods

2.1. Depth Profile Temperature Detectors

The primary tool used for this study was a custom-built 1-D vertical temperature detector (Figure 2) that enabled the recording of subsurface temperature data at high spatial and temporal resolution. The 1-D profile detectors were designed with four sensors spaced across a 50 cm distance and were set to record temperature data every 5 minutes. TMC-HD6 air/water/soil temperature sensors were utilized, which have been used in other SW-GW interaction studies (Gerecht et al., 2011; Nowinski et al., 2012;Swanson and Cardenas, 2010) because they are reliable and cost-effective. Each of the four separate temperature sensors were attached with electrical tape to a .635 cm diameter and ~60 cm length aluminum rod (c) with the sensor tips at fixed intervals of 0.1, 0.2, 0.3 and 0.5 m from a designated 0 (e) marked on the rod with tape. The sensor tips were left exposed and un-taped (b) so that they could measure temperature

effectively and accurately. Following this method, twenty-five profile detectors were constructed for deployment in both across channel and near bank transects. The four cables were taped together for neatness and ease of deployment (d). Each of these four cables connected to a Hobo U12-008 four channel Data Logger (a in Figure 2) that stored the temperature data recorded by each of the sensors. Figure 2 illustrates the configuration of a completed 1-D detector.

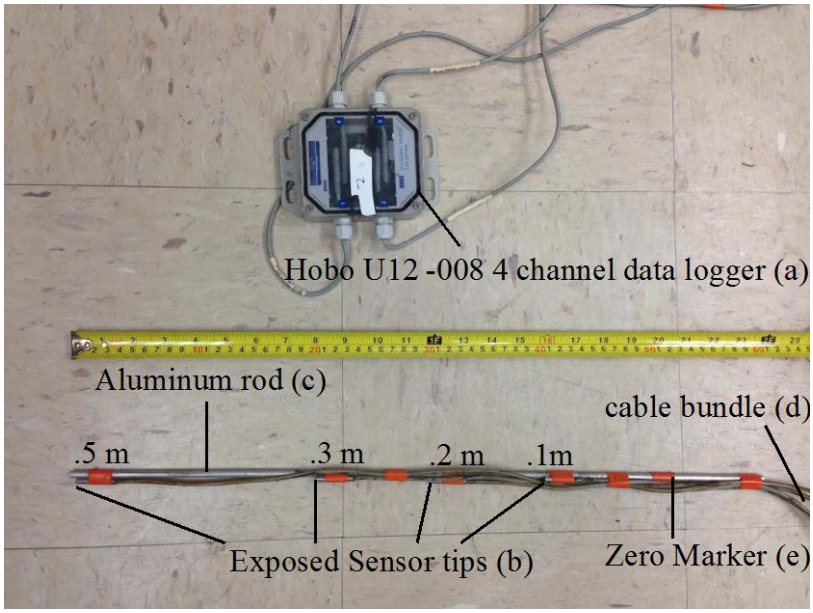

Figure 2. Annotated image of Depth Profile Temperature Detector. Letters following components correspond to in text descriptions.

The Hobo U12-008 data loggers have a reported logger accuracy of ± 2 mV ± 1% of reading for data logger-powered sensors with a resolution of 0.6 mV and an operating range of -20 to 70 °C (“HOBO U12 4-Channel External Data Logger - U12-008”). When connected to the U12 data loggers the TMC-HD6 temperature sensors have a measurement range of -40 to 50 °C in water with an accuracy of ±0.25°C from 0° to 50°C, a resolution of 0.03° at 20°C (0.05° at 68°F), and drift of <0.1°C/year. The

response time of the temperature sensors is 30 seconds in stirred water ("Air Water Soil Temp Sensor (6' cable) | Onset HOBO").

2.2. CROSS CHANNEL TRANSECT

The main research objective of this study involved collecting detailed temperature data across the entire width of the channel at the study site to see how the hyporheic zone thermal regime responded to the daily hydropeaking releases. The large size of the channel (68 m in width) and rapid daily changes in flow due to hydropeaking made data collection technically and logistically challenging. Two significant challenges included installing the temperature detectors and their cables securely enough that they wouldn't be damaged during high flow periods, and the short time windows when daylight and flow conditions allowed for working safely in the river. Spanning the river channel with instrumentation required low-profile design to ensure there was no obstruction of navigability or loss of instruments and data due to debris moving downstream during hydropeaking releases.

2.2.1 Cross Channel Transect: Temperature Profile Arrays

The limitations on deployment required pre-fabricating arrays that could be fixed to the bottom of the river before the steep daily stage increase around 12 pm. To accomplish this, six temperature arrays were constructed from twenty-four depth profile temperature detectors. The loggers and their associated depth profile temperature detectors were given ID's and organized in ascending order with different colored tape marking each end of the array to ensure deployment in ascending order. Depth profile temperature detectors (a) were spaced 2.75 m apart and the bundles of 4 cables were

taped together. Sand stakes (b) were attached to the cable bundles in-between each depth profile temperature detector so that upon deployment the cable bundles could be fixed to the river bottom and would not entrain or entangle recreational boaters or debris. The data loggers were cable tied in sets of two (c), and the two resulting groupings were loosely cable tied so that upon deployment they could be tightened to a T post in the riverbed (d). The center point of each array consisted of a T-post that served as an anchor for the loggers. Excess cable was bundled and taped into a loop (e) that could be placed over the T-post. This configuration is displayed in Figure 3.

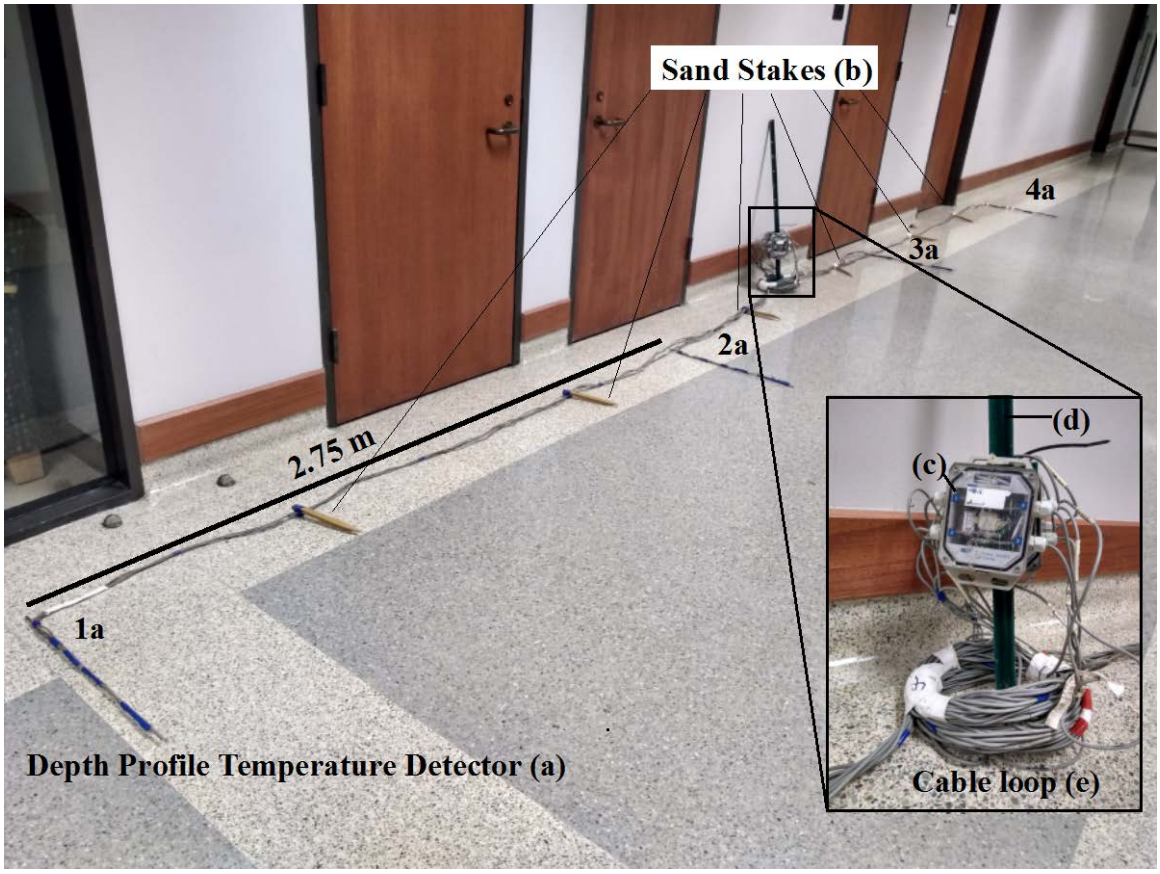

Figure 3. Annotated image showing temperature detecting array and a close up of the data loggers. (c) shows the 4 loggers cable tied together, (d) is a T post

To install the arrays in a straight line, a rope was stretched taught perpendicular to flow across the river to serve as a guide. Equipped with a weight belt and snorkel, the researcher manually installed the arrays into the riverbed with a post driver. After the first two 1-D profiles in an array were installed, the T-post was driven into the bed and the loops of bundled cable were placed over the post. The data loggers were cable tied to the T-post and the remaining two depth profile temperature detectors and their associated stakes were driven into the river bed. This process was repeated to install all of the depth profile temperature detectors 2.75 m apart spanning the 68 m from bank to bank at low stage with temperature sensors at 0.1, 0.2, 0.3, and 0.5 meters depth. Three of the depth profile temperature detectors (shown at approximately 49 m, 56 m, and 58 m) could not be driven to depth because a hard relatively impermeable clay layer was present at just over 0.3 m depth, the sensor tips at these locations were instead at 0, 0.1, and 0.3 depths. The precise locations of each depth profile temperature detector were surveyed using a

Sokkia theodolite set 610 with an accuracy of 6 degree seconds (*SOKKIA Series 10 Operator's Manual*, 2001). The data logger's clocks were synchronized and set to record at 5 minute intervals for the duration of each transect. The locations of the temperature arrays can be seen in Figure 4.

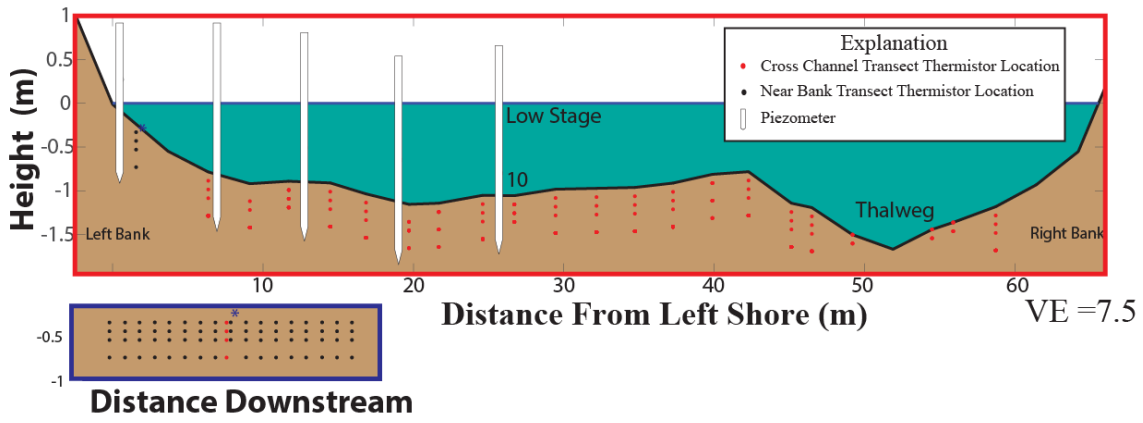

Figure 4. Diagram of field setup looking downstream showing thermistor and piezometer location and exaggerated river bathymetry (vertical exaggeration 7.5). Piezometer heights and thicknesses are not to scale.

*Location of near bank transect in relation to cross channel. Distance is downstream along left bank.

2.2.2 Cross Channel Transect: Piezometer Well Transect

In addition to the temperature profile arrays, five piezometers were installed in the riverbed to co-locate temperature measurements with specific conductance, pressure head, and additional temperature measurements (figure 4). The piezometers were spaced approximately 6 m apart starting at the left bank low water line (shoreline at low stage) to near the center of the river. The piezometers were constructed of 3.175 cm diameter PVC pipe and were driven by hand and post driver to depths of 0.5 m into the river sediment.

The PVC was screened from 0.4-0.5 m depth. The top-of-casing piezometer positions and riverbed surface elevations were surveyed using the Sokkia Theodolite Set 610. Each piezometer was instrumented with a Solinst Level Logger LTC M30 that measured specific conductance, temperature, and depth. Prior to deployment, the Solinst LTC M30 level loggers were calibrated to an accuracy of ±2% within the range of 500 - 30,000 μS/cm. The instrument accuracy for depth is ± 1.5 cm, and for temperature ±0.05ºC ("LTC Levelogger Edge"). The data logger's clocks were synchronized and set to collect data every 5 minutes. An In-Situ BaroTroll data logger was deployed at the field site to collect atmospheric temperature and pressure readings throughout the time of the study and these were subtracted from the transducer pressure readings from the piezometers so that observed changes in pressure only reflected changes in river stage. An additional monitoring well on the bank constructed of 3.175 cm diameter PVC pipes screened below the land surface and extending well into the water table was instrumented with a Solinst LTC M30 level logger. This well was used to determine average groundwater temperature and electrical conductivity.

2.2.3. Cross Channel Transect: Water Flux Estimates

Hydraulic conductivity estimates of the shallow river sediment at the field site were available from unpublished work that collected sediment samples co-located with the temperature and piezometer transect. Grain size analysis was conducted for each of the sediment samples and was used to empirically-derive K (hydraulic conductivity) values for each of the samples (Martinez 2017). The K values utilized to calculate q (specific discharge) were derived from sediment samples that were taken every 2.5m across the river at the river bed and determined using the Hazen method (Hazen, 1983).

While the samples were only collected at the surface and may not be completely representative of the 0.5 m of underlying sediment, the fluxes calculated should be considered as approximations that are likely within an order of magnitude, and importantly, this uncertainty does not affect estimates of flow direction. To calculate specific discharge, vertical hydraulic gradient is needed in conjunction with estimated hydraulic conductivity. Vertical hydraulic gradient was determined by the following equation.

$$VHG = \frac{River\ level - Piezometer\ level}{0.4m} \quad (3)$$

Where VHG is vertical hydraulic gradient and .4 meters is the distance from the sediment water interface to the top of the screened interval. The flux was determined from a modified Darcy's law considering only vertical components of specific discharge. Equation 4 is a modified version of equation 1 shown in the introduction, where the pressure gradient is replaced with the vertical hydraulic gradient

$$q = -k(VHG) \quad (4)$$

This calculation assumes one dimensional flow and does not account for multi-dimensional flow pathways. Still, it is useful in demonstrating overall flow direction and whether the river is gaining or losing water across both time and space.

2.2.4. In Stream Measurements

To measure stage and temperature, an Aqua Troll 200 was deployed in the river. The Aqua Troll 200 recorded temperature and pressure (depth) every 15 minutes. The temperature accuracy is ±0.1° C. with a resolution of 0.01° C or better and the depth accuracy is ±0.175 cm.("Aqua TROLL 200 Data Logger")To have a second in-stream

measurement of temperature, an Onset HOBO Water Temp Pro v2 with an accuracy of ±0.2°C was installed in the center of the channel cable tied to one of the T-Posts installed for the temperature sensing arrays(“HOBO Water Temperature Pro v2 Data Logger”). It logged measurements every 5 minutes.

2.3 NEARBANK TRANSECT

While this study primarily focused on the cross-channel effects of hydropeaking, the effects of hydropeaking on the near-bank hyporheic zone were also investigated. Observational (Gerecht et al., 2011) and numerical modeling studies (Wilson and Gardner, 2006; Gardner and Wilson, 2006; Shuai et al., 2017) have shown that the near-bank experiences the most significant flow changes during rising and falling stage, and suggest that this area may have disproportionate importance for net exchange during hydropeaking events. This motivated the creation of a near bank transect. The near-bank transect was easier to install because of its location out of the main flow of the river. Data loggers could be fixed onshore where debris and boaters would not disturb them. Its location relative to the river bank and the cross-channel transect is shown in Figure 4 (blue dots).

2.3.1 Near-bank Transect: Temperature Profile

Seventeen depth profile temperature detectors measured riverbed temperatures at 0.1, 0.2, 0.3 and 0.5 m depths approximately 1.5 m from the bank (here bank is used to mean the near vertical component of the river bank where it steepens dramatically). The transect spanned ~16 m going downstream. After the first depth profile temperature detector was installed 1.5 m from the bank, 1 m was measured downstream and then that

point was adjusted so that it would be 1.5 m from the bank at that location. The excess cables were bundled and placed on shore around T-posts.

2.3.2 In Stream Measurements

To measure stage and temperature, an Aqua Troll 200 was deployed in stream and cable tied and taped to a T-post driven into the stream-bed. The level logger recorded temperature, pressure and depth every 15 minutes.

2.4 DATA PROCESSING

Overall, the temperature data for both transects was of high quality with few instances of inaccurate or imprecise data, which typically resulted from damage to the sensors or cable during installation. Spikes in the temperature data (erroneous measurements) were uncommon, easy to identify, and filtered out manually. In the wells, conductivity and temperature data required no filtering or smoothing, but pressure data had some noise. The temperature data were visualized and analyzed using Mathworks Matlab to grid, interpolate, and plot the data. In Figures 7 and 11 for visualization purposes a median filter was utilized (matlab function medfilt1). Median filters smooth out noise by going element by element and replacing them with the median of surrounding elements. Additionally, linear 2-D interpolation was utilized to interpolate temperatures between measured points and create a 2-D visualization of hyporheic zone temperature. The boxplots in Figures 6 and 10 only had spikes removed and remained unfiltered. For specific discharge calculations, vertical hydraulic gradient was smoothed using a moving average (Matlab function tsmovavg) with a window set to 10 increments. Moving averages were utilized because the pressure data had some noise, this noise is

hypothesized to have come from the wells vibrating slightly with current flowing around them, as the fluctuations are not seen in the temperature or conductivity data. The moving average smoothed out the data by replacing each element with the average of the 10 elements surrounding it.

3. Results and Discussion

3.1 Cross-Channel Temperature Profiles

Subsurface temperature data for the cross-channel transect was collected over an 8-day period from 7/20-7/28 2017. The river was hydropeaked continuously over this period with daily stage fluctuations of 1-1.25m (Figure 5). During the study stream temperature was warm and had a narrow temperature range from 26.91°C to 30.70 °C while the subsurface temperatures of the shallow stream sediments had a wider range in

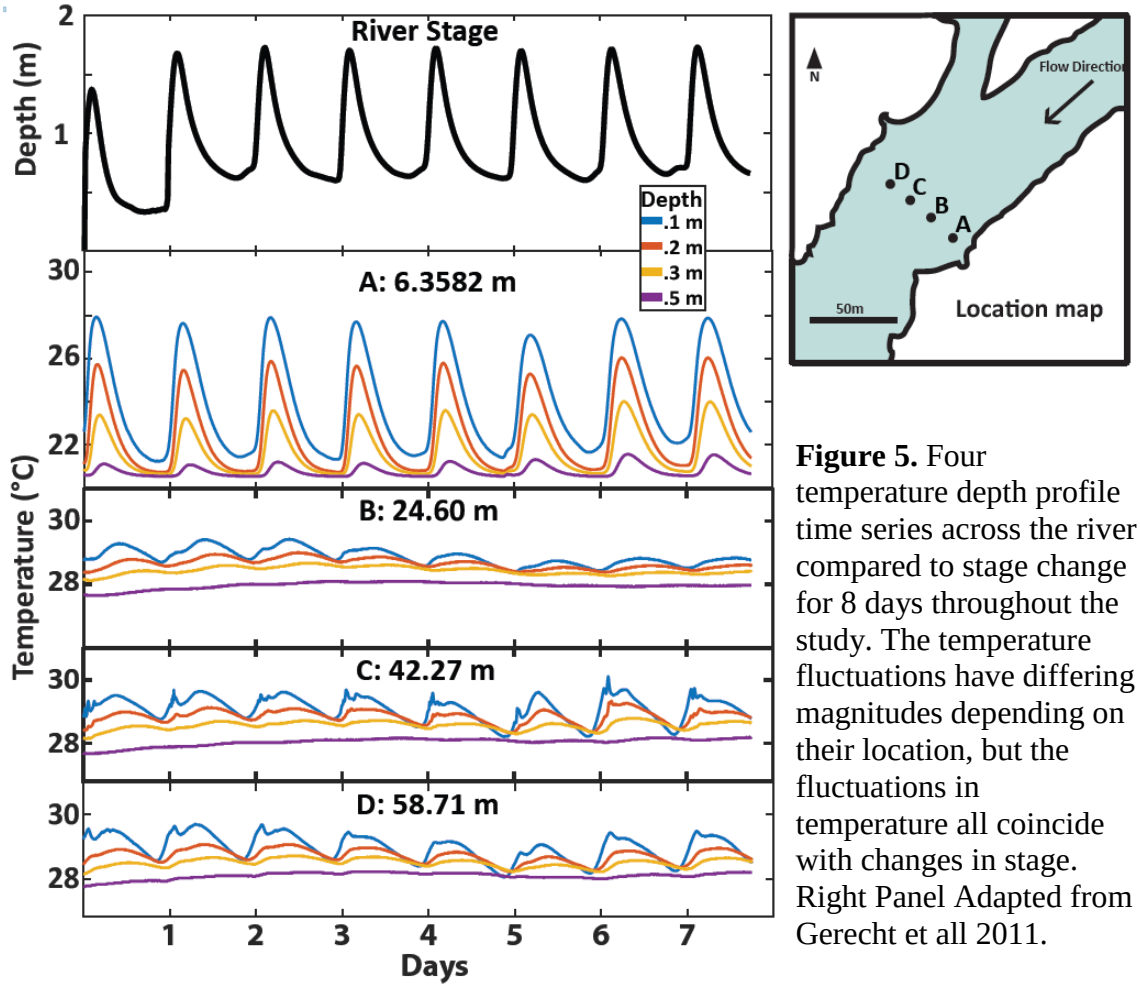

Figure 5. Four temperature depth profile time series across the river compared to stage change for 8 days throughout the study. The temperature fluctuations have differing magnitudes depending on their location, but the fluctuations in temperature all coincide with changes in stage. Right Panel Adapted from Gerecht et all 2011.

temperatures 20.53°C to 30.37°C, spanning the range of the groundwater and surface water thermal regimes. Qualitatively, the temperatures in the hyporheic zone appear to co-vary with changes in stage throughout the course of the study, and showed consistent responses day to day supporting the hypothesis that stage fluctuations cause changes in subsurface temperatures. Figure 5 shows temperature profiles at four different locations across the river and demonstrates the stage induced forcing of daily temperature fluctuations. At increasing depth in the river the temperature and magnitude of the change is smaller, and further across the river there are smaller changes in daily temperature. At location A, nearest the bank the thermal signal is seen at all depths, while at B, C and D the temperature signal is recorded in the top .3 m. Work done by Gerecht et al., (2011) demonstrated that at the study site, signature penetration by conduction alone could only reach .15 m. These results therfore support advective heat transport driven by fluid flow at all locations.

To concisely summarize the time series temperature data for all of the cross-channel data, daily ranges were calculated for all four sensors at each of the 21 locations. The calculated range (max-min daily temperature) for all of the data is summarized in

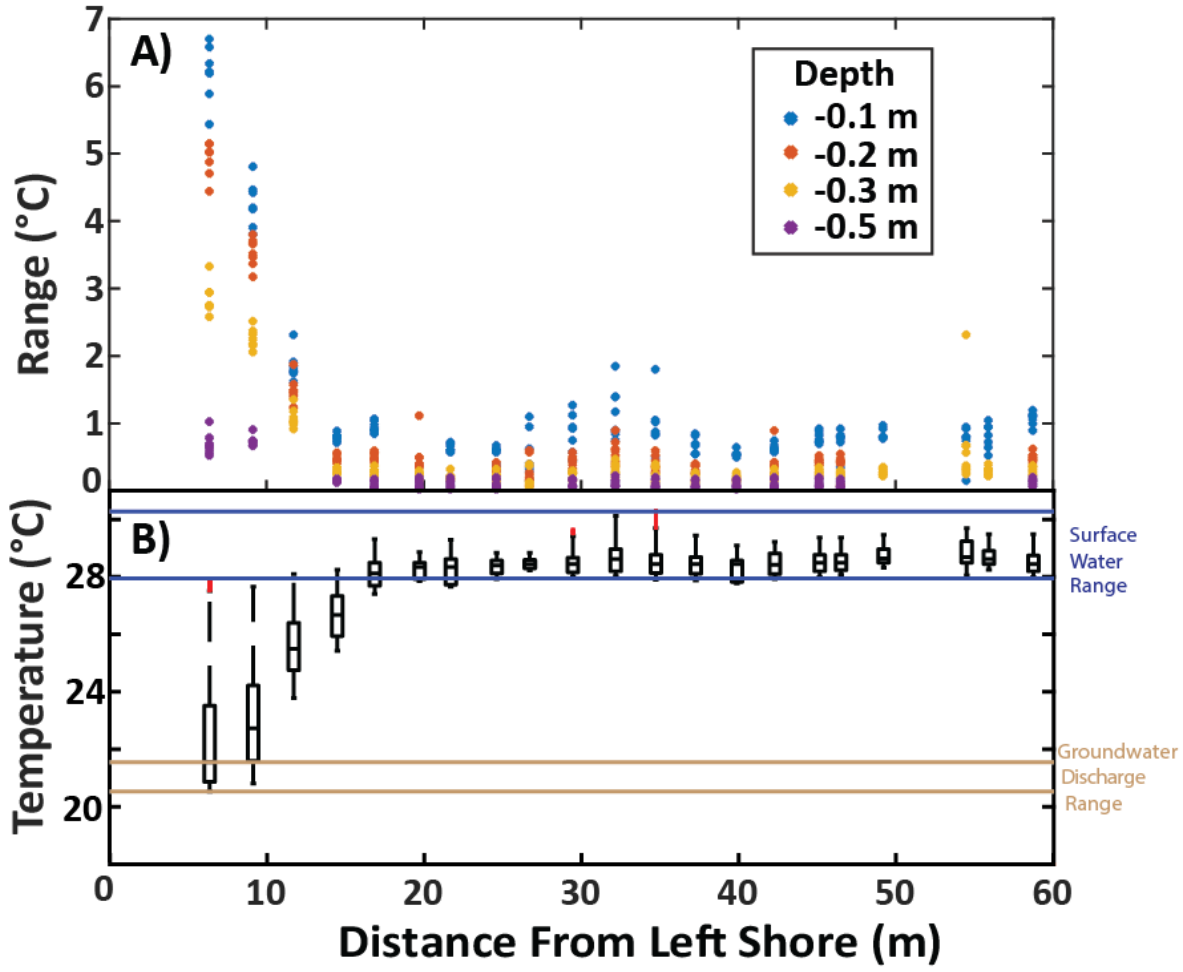

Figure 6A: Daily temperature ranges for seven days and different depths plotted against distance from the left bank. The deeper in the subsurface, the less temperature fluctuates at each location.

Figure 6B: Boxplots of temperature for 2 days (7/26-27/17) at each location across the channel. The blue lines represent the boundary minimum and maximum of surface water temperatures and the tan lines represent boundary minima and maxima of the groundwater discharge temperature range at 0.5 m depth.

Figure 6. Figure 6a shows the ranges. At 0.1 m depth the average fluctuation is 1.28 °C with a standard deviation of 1.4 °C and a maximum fluctuation of 6.7 °C. At 0.2 m depth the average fluctuation is .97°C with a standard deviation of 1.29°C and at 0.3 m depth the average fluctuation is 0.53°C with a standard deviation of 0.72°C. At 0.5 m depth the minimum fluctuation is 0.03 °C and the average across the river is 0.18 °C with a standard deviation of 0.21 °C. Within 12 m from the left back the fluctuations at all depths are higher. Isolating locations closer than 12 m at 0.1 m depth the average fluctuation is 4.10 °C with a standard deviation of 1.84 °C and at 0.5 m depth the temperature fluctuates an average of 0.72 °C with a standard deviation of 0.13°C. Beyond 12m, the subsurface temperature ranges are similar to one another with all standard deviations falling below 0.27 °C Figure 6A demonstrates these trends.

Ranges in temperatures indicate the magnitude of fluctuations at each location but do not identify the surface or ground water as the dominant forcing. A way to show the range of subsurface temperatures relative to groundwater and surface water end members is using boxplots to summarize the temperature data at each location. Figure 6b compiles two days of data, eliminating the exaggerated range displayed if all the data is displayed due to daily changes in ambient temperature. Looking at this figure, the relative influence of surface water and groundwater on the subsurface temperatures can be seen. The box plots demonstrate that beyond 19 m from shore, surface water influences the subsurface temperatures because subsurface temperatures lie entirely within the surface water range. Within 19 m, the temperature ranges indicate both surface water and ground water temperatures influence subsurface temperatures on daily scales. The fact that the daily ranges span both the groundwater discharge and surface water temperature ranges suggests groundwater-surface water mixing on daily timescales. In summary, the subsurface temperatures across the channel vary from a small range of higher

temperatures matching surface water temperatures further than 19 m from the shore to a wider range from high to low temperatures closer to the shore.

In between hydropeaks, colder water that is the near the endmember temperature of ground water rises to the surface within 12 m. Between 12 m and 19 m from the shore, there are some intermediate temperatures, while further than 19 m, the temperature of the sediments remain consistently warm. During a hydropeaking cycle (defined as low stage to high stage back to low stage), locations within 19 m of the bank show subsurface temperatures respond to and experience varying proportions of the endmember temperatures. At the initiation of a hydropeak, the subsurface temperatures are similar to the resting distribution of temperatures. As the hydropeak progresses there is a rapid increase in temperatures near the bank, and soon after the hydropeak the temperatures in the first 0.5 m as measured all exhibit influence from surface water. Afterwards the cooler groundwater temperatures return at the locations near the bank. This rapid disappearance of the warm surface water temperatures near the bank implies a resumption of groundwater upwelling. Further into the channel, the temperatures remain consistently warm and there are only subtle changes in hyporheic sediment temperatures throughout the course of a hydropeak. This is demonstrated in figure 7. At the right bank, the upwelling, cooler signal is not seen. This likely indicates a deeper groundwater table and potential losing conditions locally.

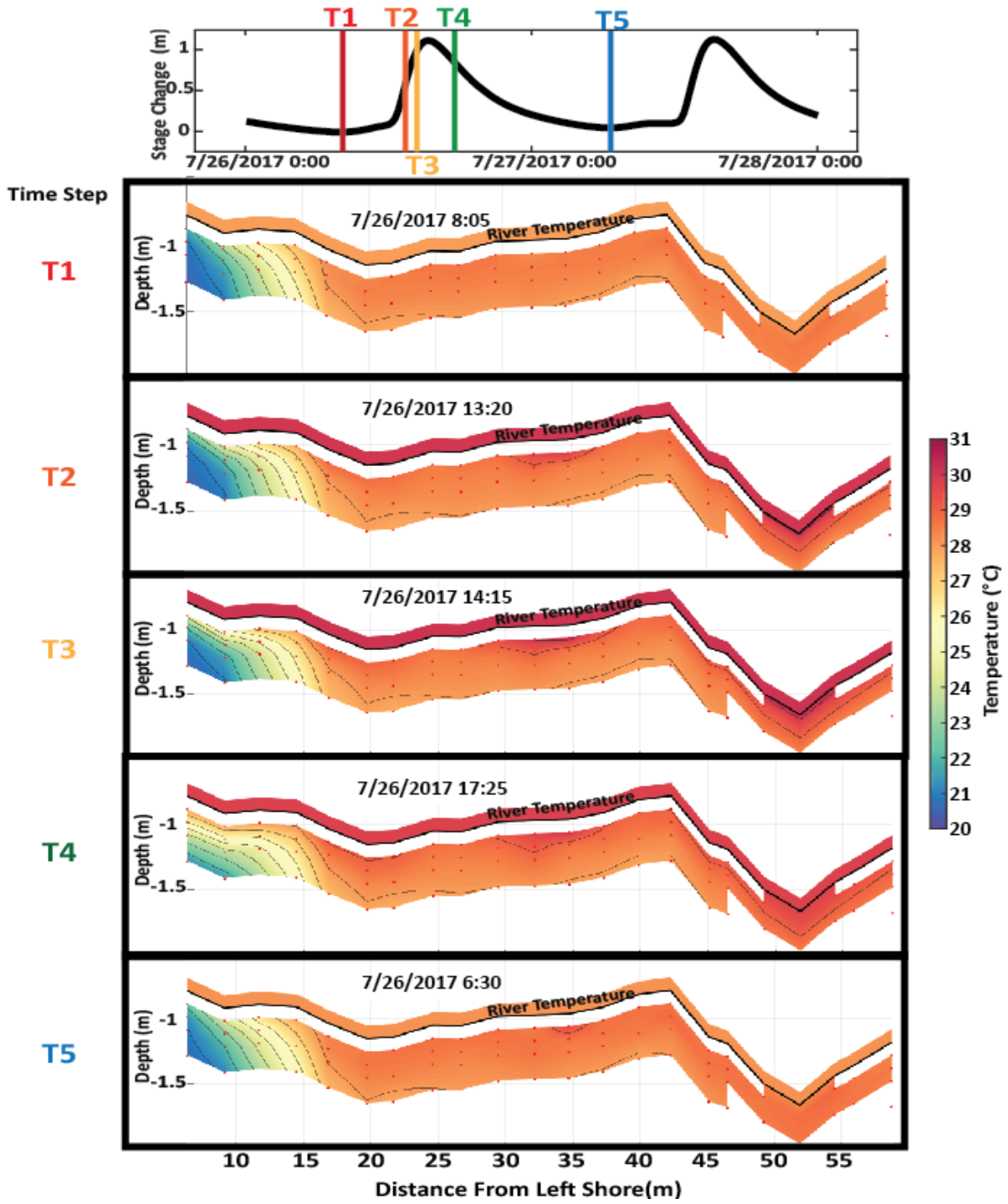

Figure 7. 2D temperature profiles across the river throughout the course of a hydro peaking event. T1 shows low stage and the steady resting distribution of temperatures. T2 and T3 show the temperature distributions just before a hydropeak. T4 shows just after a hydropeak. T5 is a return to steady resting distribution of temperature. The temperature increases in the subsurface is most extreme near the bank in T4, while through all time steps the sediments beyond 12 m see little change.

Differing temperature responses to hydropeaking were based on location and are demonstrated in both the range and temperature time series analysis. Temperature ranges were high and influenced by both surface and groundwater near the left bank, yet diminished to surface water ranges across the width of the river. The right bank did not show influence from groundwater temperatures. Jackson et al., (2007) and Hill and Hawkins (2014) both state temperature's importance in determining benthic macroinvertebrate assemblage and widescale studies determining the effect of different stressors on macroinvertebrate assemblages utilize stream temperature as a variable (Meador et al., 2008; Carlisle et al., 2007). Beyond macroinvertebrate assemblages, temperature is a controlling factor for nutrient processing associated with microbial communities and biofilms (Boano et al., 2014). These findings show that over the course of 8 days with a stream temperature range of 3.9°C subsurface temperatures experience a much larger range of 9.83°C. Stream temperature remains an important variable, but in hydropeaked gaining systems the range of temperature in the river will usually be smaller than the range of temperatures in the nearbank benthic habitat. This implies that as an environmental indicator, surface water temperatures may be insufficient for determining aquatic habitat suitability in hydropeaked systems, especially for benthic macroinvertebrates and hyporheic biofilms which reside in the subsurface. Gradients of nutrient and chemical availability will be highly changing and evolving near the bank and discharge zones, while further in the river temperatures are more static despite large stage fluctuations.

3.2 Across Channel In-stream Piezometer Data

Wells in the stream provided head, conductivity, and temperature data to corroborate with the temperature data obtained in cross section. In some cases, the additional chemical and conductivity measurements revealed patterns not demonstrated through temperature alone. Using pressure head data in the piezometers with head from the river surface elevation, vertical head gradients were calculated to estimate vertical flux rates.

Locations near the bank experienced flux and gradient reversals that co-varied with river stage. The only two locations that experienced gradient reversals and a change in the direction of flux from into the bank to out of the bank were at 0.56 and 6.9 m. Beyond this distance, the gradients and fluxes did not change with stage, and remained relatively constant throughout each hydropeaking event. The largest positive (out of bank) and negative (into bank) fluxes were measured at 6.9 m from the shore, with fluxes

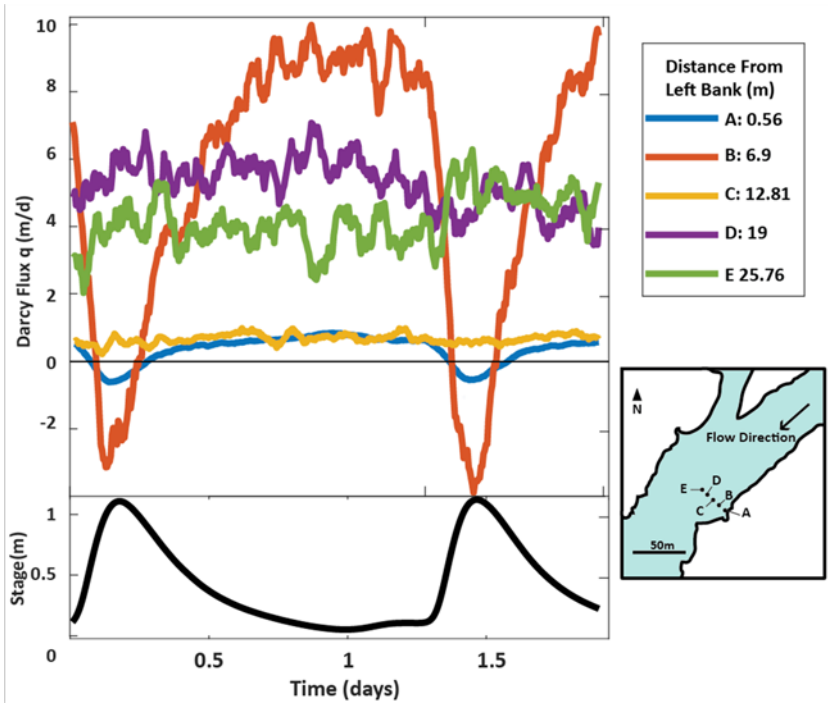

Figure 8. Estimated fluxes throughout the course of 2 flood pulses. Two Locations near the bank (0.56 and 6.9 m) experienced flux and gradient reversals that co varied with river stage. The remaining 3 wells did not change with stage, and remained relatively constant throughout the course of the study. This pattern is consistent with the thermal data presented in figure 7 and the electrical conductivity presented in figure 8 which show similar spatial trends of response to stage.

out of the bank reaching 10 m/d specific discharge (also known as Darcy flux) and dropping to nearly -3 m/day. Sediments near the bank recorded much smaller discharge despite a higher vertical head gradient due to lower hydraulic conductivity values. These results are presented in Figure 8. At the study site, groundwater and surface water have different specific conductance values. Throughout the course of the study, the groundwater well in the bank measured an average of 1237 µS/cm. The river, while well homogenized at any given instant, has a specific conductance that varies through time.

Other workers at this field site have found the average specific conductance of the river to be 550 µS/cm (Stephen Ferencz, Personal Communication). Using these values as pure groundwater and pure surface water endmembers in a ratio allowed the conductivity values collected in the river piezometers to determine the percent contribution of each endmember during hydropeaking events. This calculation is a rough approximation, as it assumes constant and unchanging conductivity values for the groundwater and surface water endmembers. Additionally the water previously in the piezometer is mixing with

the water coming in through the slots as it changes in the sediments, and is therefore only an approximate measure of the specific conductance at any given time. While a well in the bank was utilized to determine an average groundwater specific conductance, the highest measured specific conductance was actually in one of the river piezometers and

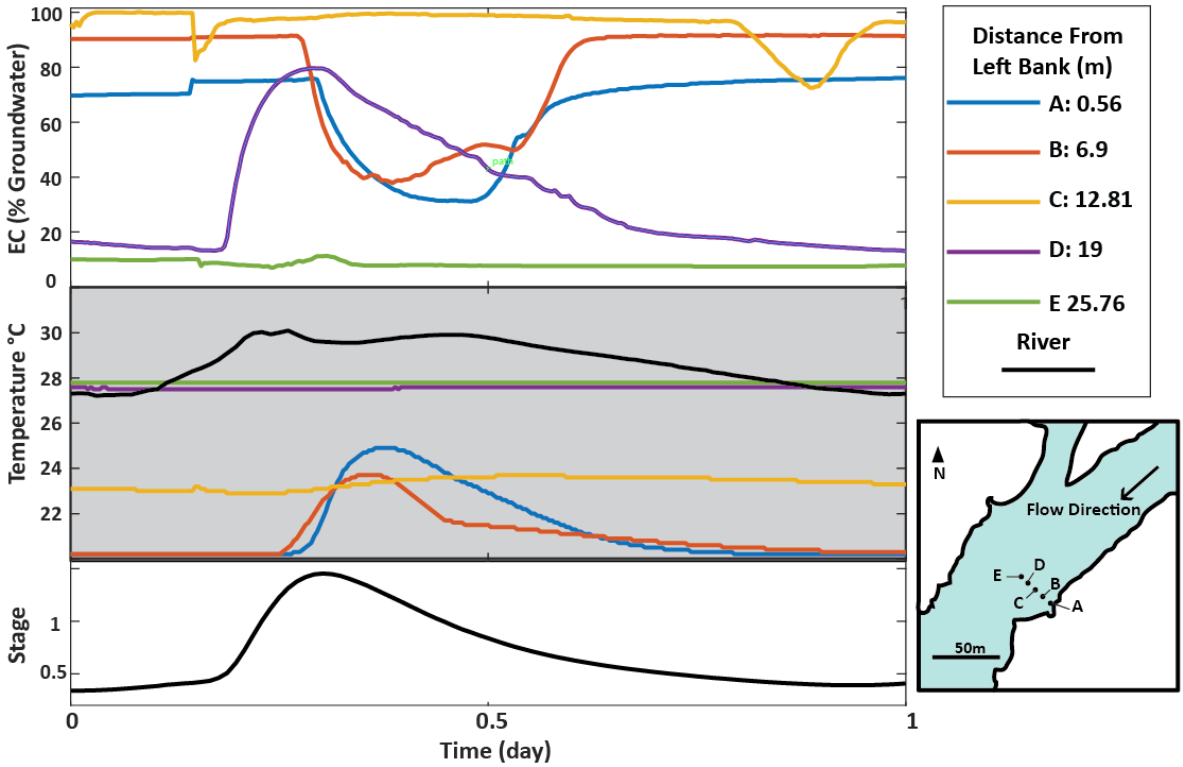

Figure 9. Relationship between specific conductance (percent groundwater assuming pure GW specific conductance = 1287 µS/cm and surface water specific conductance =550 µS/cm), temperature, and stage for the 5 piezometers located from .56 m from the bank to 25.76 m into the river. Specific conductance values indicate mixing, as well as some trends that are not displayed in the thermal data. Wells A and B are anti-correlated with stage changes, demonstrating surface water infiltration into the subsurface near the bank at high stage. Well C does not vary with stage change and is almost purely groundwater, while well D co varies with stage but rises to a higher percent groundwater which is the opposite of what is expected. Well E is nearly all surface water all the time, and does not vary with

was 1287 µS/cm for the period shown, so this value was used for a pure groundwater endmember. Figure 9 shows the results from this end-member analysis. At 0.5 and 7 meters from the bank, flood pulses cause a mixing of surface and groundwater, and each

location goes from being predominantly groundwater to predominantly surface water. This is shown in the temperature profile data. The well at 13 m has a relatively constant electrical conductivity, and is close to 100% groundwater at all times. The only exception are small dips at low stage prior to a hydropeak.

At 19 m, an unexpected pattern is displayed where rise in conductivity and groundwater percent are seen with a rise in stage. Lastly, at 26m the hyporheic water is nearly all surface water, and sees no effects of the hydropeak. While this end-member analysis is a coarse estimate, it shows bulk behavior of hyporheic composition and degree of GW-SW mixing in response to hydropeaking events.

In addition to providing estimates of GW-SW mixing, the pressure data from the piezometer measurements help explain the difference in temperature responses observed across the channel. Pressure gradients and fluxes reverse throughout flood pulses within 12 m from the bank, while further out, there is a minimal change in head gradients despite large fluctuations in stage. Time varying loading in an aquifer results in changing stresses on the aquifer, and can lead to diminished recharge because of increasing pore pressure due to surficial load (Reeves et al., 2000). This has been extensively documented in tidal systems (Befus et al., 2013; Cardenas et al., 2015; Reeves et al., 2000; Gardner and Wilson, 2006) and recent work has shown the concept applied to freshwater systems (Shuai et al., 2017). Modeling based on the study site incorporating this loading effect have shown results consistent with our field observations and temperature and head gradients measured in this study serve as evidence for this process (Shuai et al., 2017). Changes in stage drive exchange near the banks while across the river despite dynamic conditions loading results in largely static gradient and flow conditions in the bed. Measuring electrical conductance demonstrates patterns not seen in the pressure and temperature fields, and while these measurements were not a main focus of the study,

they likely demonstrate the presence of multiple flow regimes and non-vertical and one dimensional flow fields. The measurement in the piezometer at 19 m demonstrates a trend that would not be seen in only temperature data, as in the well during a hydropeak temperatures rise with the river fluctuation, yet instead of low conductivity values high values are measured. This demonstrates what could be interpreted as hyporheic groundwater with a longer residence time and non-vertical flow pathway that remains in the bed long enough to be warmed up through conduction.

3.3 Near Bank Temperature Profiles

Near bank temperatures 1.5 m from the left shore followed the trend observed in the cross channel transect of decreasing range with depth. At 0.5 m depth the minimum fluctuation is 0.09 °C and the average across the river is 1.84 °C with a standard deviation of 0.7 °C. In contrast, at 0.1 m depth the average fluctuation is 5.77 °C with a standard deviation of 0.95°C and a maximum fluctuation of 7.4 °C. These values fit in with the trends observed in Figures 6a and 6b.The near bank values also fit the trend of increasing range with proximity to the bank. There are no observable trends/differences moving downstream, which validates the cross channel transect as representative of this reach of river on the scale of meters up and downstream. The data is displayed in Figure 10a. Figure 10b displays the data for 2 days in boxplots grouped by location. Each boxplot extends from within the groundwater range into the surface water range, which indicates influence from both the surface water and ground-water temperatures. The boxplots display no trends moving downstream, and compared to figure 6b fit in the trend set and would plot as expected from the across channel investigation due to their distance from the shore.

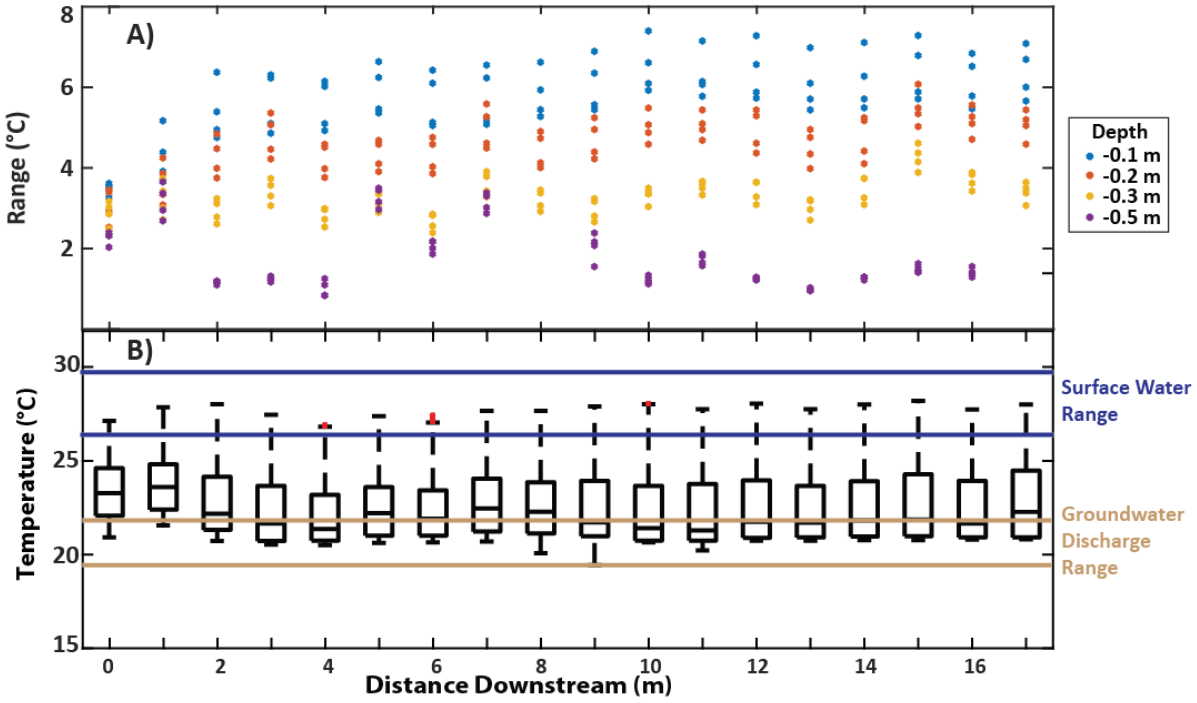

Figure 10 A: Daily temperature ranges for 6/22-26/17 at four depths 1.5 m from the shore moving downstream along the bank. The ranges matches the trends found in plot 6a and 6b as all of these locations are closer to the bank and display the same large range consistent with being near the bank. There is a consistent scatter to the points, suggesting that there are no differing trends moving downstream. There is a consistent trend of decreasing range with depth.

Figure 10 B: Box plots of temperature range moving downstream 1.5 m from the bank. The blue lines represent the boundary minimum and maximum of surface water temperatures, the tan lines represent boundary minima and maxima of the groundwater discharge temperature range at .5 m depth. The boxplots extend through both ranges in all cases, which indicates influence of both surface water and groundwater in the first .5 m at all locations.

The subsurface temperatures near the bank throughout the course of a hydropeak show uniform response moving downstream, and the penetration of the thermal signal

reaches all the way to 0.5 m depth. In between peaks, cool groundwater endmember temperatures dominate the subsurface temperatures. Figure 11 shows snapshots of the subsurface temperatures throughout the course of a hydropeak, demonstrating the

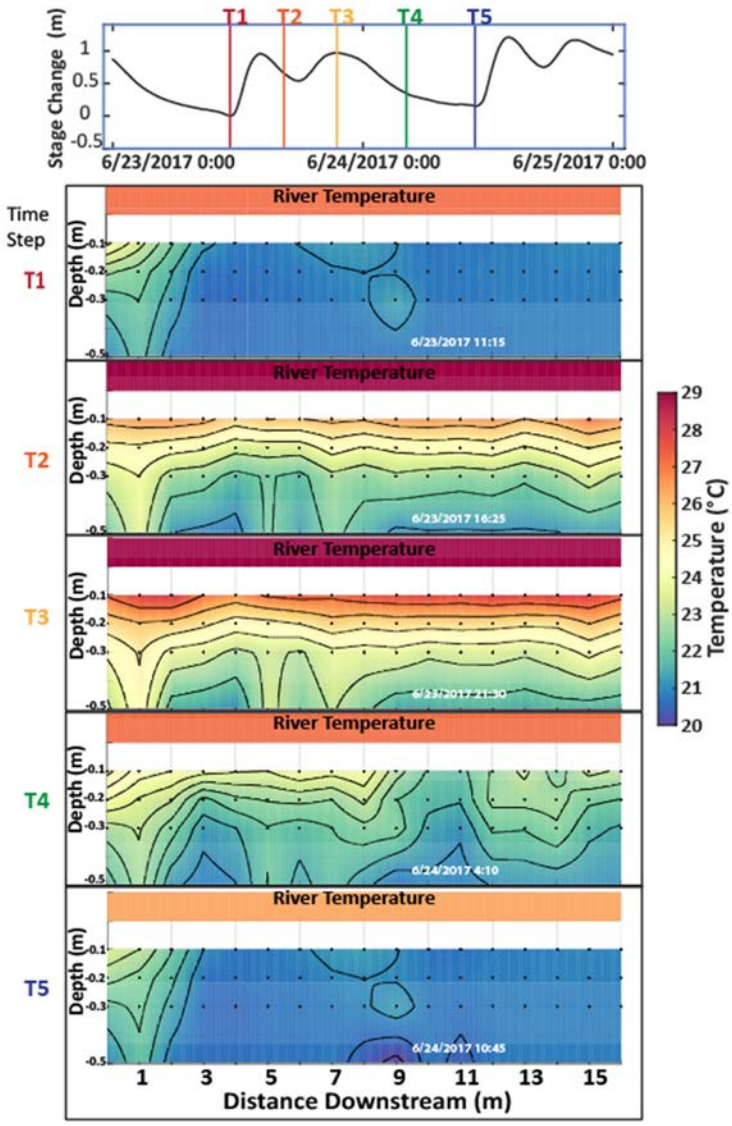

Figure 11. Shows 2D temperature profiles at different time slices along the bank 1.5 m from the shore moving downstream. The temperature distributions follow the trend established across channel transect shown in figure 7, of reversals of flow and surface water infiltration with proximity to the bank. T1 shows between hydropeaks, with cool groundwater dominating the subsurface temperature profile. T2 is just after a peak showing some infiltration, T3 is at a peak and has surface water temperatures affecting nearly the entire first 50 cm of the subsurface, T4 is the tail of a hydropeak and shows cool groundwater temperatures returning, and T5 is at the end of a hydropeak and shows a temperature distribution similar to that in T1.

penetration of warm surface water signals into the subsurface, and the recovery of cooler temperatures matching cooler groundwater signals.

The downstream transect demonstrated consistency and minimal changes in temperature response as a function of distance downstream. Since pressure measurements explained differences in temperature, it can be inferred that the findings are not isolated to the 2d cross section, but can be generalizable upstream and downstream as well.

4. Conclusions

The effects of hydropeaking on the temperature regime and surface and groundwater interactions in a large regulated river were investigated by measuring two temperature depth profiles, one near the bank moving downstream and the other across the width of the river. Piezometers allowed for the additional measurement of head gradients and specific conductance measurements of hyporheic water. Near a gaining bank hydropeaking induces increased temperature ranges and groundwater surface water interactions while further away from the bank temperature profiles and pressure gradients remain more close to static. Results from this study indicate measurements of surface water temperature alone may not be sufficient to show disturbance from hydropeaking as temperature ranges are higher in the streambed than in the river, which is an important ecotone and a biologically significant component of the system. Flux and gradient reversals explain the temperature distribution and are consistent with findings investigating loading effects in intertidal zones, where the weight of water associated with tidal increase is analogous to the rapid stage change caused by hydropeaking. This effect has been successfully incorporated into models at the study site, and the model results match physical observations. Electrical conductivity data suggests the presence of multiple scales of flow pathways, revealing patterns not seen in temperature profiles. Down-stream results indicate that cross channel observations can be extrapolated downstream on m scales despite the high prevalence of heterogeneity in the river. Future recommendations in the investigation of hyporheic zones and dam regulation include investigations further quantifying microbial and benthic macroinvertebrate assemblage and response to the presence of static and dynamic habitat created by hydropeaking, as

well as investigation into signals of the multi-dimensional flow components of hyporheic exchange.

Works Cited

Air Water Soil Temp Sensor (6’ cable) | Onset HOBO, http://www.onsetcomp.com/products/sensors/tmc6-hd (accessed February 2018).

Allan, J.D., and Castillo, M.M., 2007, Stream Ecology: Structure and function of running waters: Springer Netherlands, //www.springer.com/us/book/9781402055829 (accessed February 2018).

Anderson, M.P., 2005, Heat as a Ground Water Tracer: Ground Water, v. 43, p. 951–968, doi: 10.1111/j.1745-6584.2005.00052.x.

Aqua TROLL 200 Data Logger In-Situ, https://in-situ.com/products/water-level-monitoring/aqua-troll-200-data-logger/ (accessed February 2018).

Arntzen, E.V., Geist, D.R., and Dresel, P.E., 2006, Effects of fluctuating river flow on groundwater/surface water mixing in the hyporheic zone of a regulated, large cobble bed river: River Research and Applications, v. 22, p. 937–946, doi: 10.1002/rra.947.

Befus, K.M., Cardenas, M.B., Erler, D.V., Santos, I.R., and Eyre, B.D., 2013, Heat transport dynamics at a sandy intertidal zone: Water Resources Research, v. 49, p. 3770–3786, doi: 10.1002/wrcr.20325.

Boano, F., Harvey, J.W., Marion, A., Packman, A.I., Revelli, R., Ridolfi, L., and Wörman, A., 2014, Hyporheic flow and transport processes: Mechanisms, models, and biogeochemical implications: Reviews of Geophysics, v. 52, p. 603–679, doi: 10.1002/2012RG000417.

Burkholder, B.K., Grant, G.E., Haggerty, R., Khangaonkar, T., and Wampler, P.J., 2008, Influence of hyporheic flow and geomorphology on temperature of a large, gravel-bed river, Clackamas River, Oregon, USA: Hydrological Processes, v. 22, p. 941–953, doi: 10.1002/hyp.6984.

Cardenas, M.B., Bennett, P.C., Zamora, P.B., Befus, K.M., Rodolfo, R.S., Cabria, H.B., and Lapus, M.R., 2015, Devastation of aquifers from tsunami-like storm surge by Supertyphoon Haiyan: Geophysical Research Letters, v. 42, p. 2844–2851, doi: 10.1002/2015GL063418.

Carlisle, D.M., Meador, M.R., Moulton, S.R., and Ruhl, P.M., 2007, Estimation and application of indicator values for common macroinvertebrate genera and families of the United States: Ecological Indicators, v. 7, p. 22–33, doi: 10.1016/j.ecolind.2005.09.005.

Chapra, S.C., 2008, Surface water-quality modeling: Long Grove, IL, Waveland press.

Conant, B., 2004, Delineating and quantifying ground water discharge zones using streambed temperatures: Ground Water, v. 42, p. 243–257, doi: 10.1111/j.1745-6584.2004.tb02671.x.

Curry, R., Gehrels, J., Noakes, D., and Swainson, R., 1994, Effects of River Flow Fluctuations on Groundwater Discharge Through Brook Trout, Salvelinus-Fontinalis, Spawning and Incubation Habitats: Hydrobiologia, v. 277, p. 121–134, doi: 10.1007/BF00016759.

Dahm, C.N., Grimm, N.B., Marmonier, P., Valett, H.M., and Vervier, P., 1998, Nutrient dynamics at the interface between surface waters and groundwaters: Freshwater Biology, v. 40, p. 427–451, doi: 10.1046/j.1365-2427.1998.00367.x.

Ebersole, J.L., Liss, W.J., and Frissell, C.A., 2003, Thermal heterogeneity, stream channel morphology, and salmonid abundance in northeastern Oregon streams: Canadian Journal of Fisheries and Aquatic Sciences, v. 60, p. 1266–1280, doi: 10.1139/F03-107.

Findlay, S., 1995, Importance of surface-subsurface exchange in stream ecosystems: The hyporheic zone: Limnology and Oceanography, v. 40, p. 159–164, doi: 10.4319/lo.1995.40.1.0159.

Gardner, L.R., and Wilson, A.M., 2006, Comparison of four numerical models for simulating seepage from salt marsh sediments: Estuarine, Coastal and Shelf Science, v. 69, p. 427–437, doi: 10.1016/j.ecss.2006.05.009.

Gerecht, K.E., Cardenas, M.B., Guswa, A.J., Sawyer, A.H., Nowinski, J.D., and Swanson, T.E., 2011, Dynamics of hyporheic flow and heat transport across a bed-to-bank continuum in a large regulated river: Water Resources Research, v. 47, p. W03524, doi: 10.1029/2010WR009794.

Hancock, P.J., 2002, Human Impacts on the Stream–Groundwater Exchange Zone: Environmental Management, v. 29, p. 763–781, doi: 10.1007/s00267-001-0064-5.

Hawkins, C.P., Hogue, J.N., Decker, L.M., and Feminella, J.W., 1997, Channel morphology, water temperature, and assemblage structure of stream insects: Journal of the North American Benthological Society, v. 16, p. 728–749, doi: 10.2307/1468167.

Hazen, A., 1983, Some physical properties of sand and gravel with special reference to their use in filtration: 24th Ann, Rep., Mass. State Board of Health, Boston, 1983,.

Hester, E.T., and Doyle, M.W., 2011, Human Impacts to River Temperature and Their Effects on Biological Processes: A Quantitative Synthesis1: JAWRA Journal of the American Water Resources Association, v. 47, p. 571–587, doi: 10.1111/j.1752-1688.2011.00525.x.

Hill, R.A., and Hawkins, C.P., 2014, Using modelled stream temperatures to predict macro-spatial patterns of stream invertebrate biodiversity: Freshwater Biology, v. 59, p. 2632–2644, doi: 10.1111/fwb.12459.

HOBO U12 4-Channel External Data Logger - U12-008, http://www.onsetcomp.com/products/data-loggers/u12-008 (accessed February 2018).

HOBO Water Temperature Pro v2 Data Logger, http://www.onsetcomp.com/products/data-loggers/u22-001 (accessed February 2018).

Hucks Sawyer, A., Bayani Cardenas, M., Bomar, A., and Mackey, M., 2009, Impact of dam operations on hyporheic exchange in the riparian zone of a regulated river: Hydrological Processes, v. 23, p. 2129–2137, doi: 10.1002/hyp.7324.

Jackson, H.M., Gibbins, C.N., and Soulsby, C., 2007, Role of discharge and temperature variation in determining invertebrate community structure in a regulated river: River Research and Applications, v. 23, p. 651–669, doi: 10.1002/rra.1006.

Jones, N.E., 2014, The Dual Nature of Hydropeaking Rivers: Is Ecopeaking Possible? River Research and Applications, v. 30, p. 521–526, doi: 10.1002/rra.2653.

Łaszewski, M., 2016, Relationships between environmental metrics and water temperature: a case study of Polish lowland rivers: Water and Environment Journal, v. 30, p. 143–150, doi: 10.1111/wej.12173.

LCRA dams form the Highland Lakes, https://www.lcra.org/water/dams-and-lakes/Pages/default.aspx (accessed March 2018).

LTC Levelogger Edge, https://www.solinst.com/products/dataloggers-and-telemetry/3001-levelogger-series/ltc-levelogger/datasheet.php (accessed February 2018).

Meador, M.R., Carlisle, D.M., and Coles, J.F., 2008, Use of tolerance values to diagnose water-quality stressors to aquatic biota in New England streams: Ecological Indicators, v. 8, p. 718–728, doi: 10.1016/j.ecolind.2008.01.002.

Nilsson, C., Reidy, C.A., Dynesius, M., and Revenga, C., 2005, Fragmentation and Flow Regulation of the World's Large River Systems: Science, v. 308, p. 405–408, doi: 10.1126/science.1107887.

Nowinski, J.D., Cardenas, M.B., Lightbody, A.F., Swanson, T.E., and Sawyer, A.H., 2012, Hydraulic and thermal response of groundwater–surface water exchange to flooding in an experimental aquifer: Journal of Hydrology, v. 472–473, p. 184–192, doi: 10.1016/j.jhydrol.2012.09.018.

Parkinson, E.A., Lea, E.V., Nelitz, M.A., Knudson, J.M., and Moore, R.D., 2016, Identifying Temperature Thresholds Associated with Fish Community Changes in British Columbia, Canada, to Support Identification of Temperature Sensitive Streams: River Research and Applications, v. 32, p. 330–347, doi: 10.1002/rra.2867.

Poff, N.L., Allan, J.D., Bain, M.B., Karr, J.R., Prestegaard, K.L., Richter, B.D., Sparks, R.E., and Stromberg, J.C., 1997, The natural flow regime: A paradigm for river conservation and restoration: BioScience, v. 47, p. 769–784.

Poole, G.C., and Berman, C.H., 2001, An ecological perspective on in-stream temperature: natural heat dynamics and mechanisms of human-caused thermal degradation: An Ecological Perspective on In-Stream Temperature journalArticle ISSN0364-152X, doi: 10.1007/s002670010188.

Rau, G.C., Andersen, M.S., and Acworth, R.I., 2012, Experimental investigation of the thermal dispersivity term and its significance in the heat transport equation for flow in sediments: Water Resources Research, v. 48, doi: 10.1029/2011WR011038.

Rau, G.C., Andersen, M.S., McCallum, A.M., Roshan, H., and Acworth, R.I., 2014, Heat as a tracer to quantify water flow in near-surface sediments: Earth-Science Reviews, v. 129, p. 40–58, doi: 10.1016/j.earscirev.2013.10.015.

Reeves, H.W., Thibodeau, P.M., Underwood, R.G., and Gardner, L.R., 2000, Incorporation of Total Stress Changes into the Ground Water Model SUTRA: Ground Water, v. 38, p. 89–98, doi: 10.1111/j.1745-6584.2000.tb00205.x.

Shuai, P., Cardenas, M.B., Knappett, P.S.K., Bennett, P.C., and Neilson, B.T., 2017, Denitrification in the banks of fluctuating rivers: The effects of river stage amplitude, sediment hydraulic conductivity and dispersivity, and ambient groundwater flow: Water Resources Research, v. 53, p. 7951–7967, doi: 10.1002/2017WR020610.

SOKKIA Series 10 Operator’s Manual, 2001, 260-63 HASE, ATSUGI, KANAGAWA, 243-0036 JAPAN, SOKKIA CO, LTD, 144 p., https://cn.sokkia.com/sites/default/files/sc_files/downloads/set_10_series_operators_manual_-_4th_ed_0.pdf (accessed February 2018).

Swanson, T.E., and Cardenas, M.B., 2010, Diel heat transport within the hyporheic zone of a pool-riffle-pool sequence of a losing stream and evaluation of models for fluid flux estimation using heat: Limnology and Oceanography, v. 55, p. 1741–1754, doi: 10.4319/lo.2010.55.4.1741.

Trauth, N., Musolff, A., Knoeller, K., Kaden, U.S., Keller, T., Werban, U., and Fleckenstein, J.H., 2018, River water infiltration enhances denitrification efficiency in riparian groundwater: Water Research, v. 130, p. 185–199, doi: 10.1016/j.watres.2017.11.058.

U.S. Geological Survey, 2018, National Water Information System data available on the World Wide Web (Water Data for the Nation):, https://waterdata.usgs.gov/nwis/annual/?referred_module=sw&site_no=08158000&por_08158000_136117=1389,00060,136117,1898,2018&start_dt=1900&end_dt=2017&year_type=W&format=html_table&da

te_format=YYYY-MM
DD&rdb_compression=file&submitted_form=parameter_selection_list (accessed March 2018).

Vervier, P., Gibert, J., Marmonier, P., and Doleolivier, M., 1992, A Perspective on the Permeability of the Surface Fresh-Water-Groundwater Ecotone: Journal of the North American Benthological Society, v. 11, p. 93–102, doi: 10.2307/1467886.

White, D.S., 1993, Perspectives on Defining and Delineating Hyporheic Zones: Journal of the North American Benthological Society, v. 12, p. 61–69, doi: 10.2307/1467686.

Vita

Sebastian Muñoz grew up in The Woodlands, Texas, and attended the Science Academy at the Woodlands College Park High School. He began his path at UT as a Plan II and Chemistry double major, and switched to Environmental Science after a life changing summer guiding rafts down the Rio Grande in northern New Mexico. He helped found the Longhorn Stream Team, UT's citizen science chapter focused on conservation of Texas water resources, and served as their river operation manager for several years. He is finishing with a Hydrogeology and Plan II double major, and has found that this combination has allowed him to spend the most time thinking about rivers. He will be working on the Rogue and Klamath rivers in Oregon during the summer of 2018, and is considering returning to graduate school after some time spent kayaking and working as a raft guide.

Permanent Email: smunoz1212@gmail.com

This Thesis was typed by Sebastian Muñoz